Sulfonated poly(arylene ether nitrile)-based composite membranes enhanced with Ca^{2+} bridged carbon nanotube-graphene oxide networks

Mengna Feng (fengmengnafwch@126.com)
Yancheng Institute of Technology
Yan Ma
University of Electronic Science and Technology of China
JiaJia Chang
Yancheng Institute of Technology
Jing Lin
Yancheng Teachers University
Ying Xu
Huaiyin Institute of Technology
Yan Feng
Shenzhen Extender Co., Ltd
Yumin Huang
University of Electronic Science and Technology of China
Luoju Hua
Yancheng Institute of Technology

Research Article

Keywords: Sulfonated poly(arylene ether nitrile), Proton exchange membrane, Graphene oxide, Multi-walled carbon nanotubes, Three-dimensional network structure

Posted Date: January 14th, 2022

DOI: https://doi.org/10.21203/rs.3.rs-1237693/v1

Version of Record: A version of this preprint was published at Journal of Inorganic and Organometallic Polymers and Materials on March 8th, 2022. See the published version at https://doi.org/10.1007/s10904-022-02275-3.

Abstract

As the core component of proton exchange membrane fuel cell, proton exchange membranes (PEM) have attracted much attention of researchers. To trade-off the proton conduction, dimensional stability and anti-oxidation ability, graphene oxide (GO) and acidized multi-walled carbon nanotubes (MWCNT) using calcium ion as coordination bridge (GO-Ca^{2+}-MWCNT) was synthesized, and then incorporating into sulfonated poly(arylene ether nitrile) (SPEN) to fabricate SPEN/GO-Ca^{2+}-MWCNT organic-inorganic composite membranes by solution-casting method and explore the influence of varying loading on performances as PEM. It was found that the proton conductivity of the composite membranes was higher than that of SPEN, while maintaining better dimensional stability, excellent anti-oxidation ability and good mechanical properties. All of these were attributed to the formation of three-dimensional structure between GO and MWCNT bridged by Ca^{2+}. Particularly, the SPEN/GO-Ca^{2+}-MWCNT-1 composite membrane exhibited excellent tensile strength of 71.45 MPa, better thermal stability as well as high proton conductivity (0.054 S/cm at 30 ℃, and 0.193 S/cm at 90 ℃), above 10^{-2} S/cm, satisfying the requirement of fuel cells. All in all, the results indicate that the filler with three-dimensional network structure can effectively improve the performances of SPEN, and the prepared composite membranes show potential applications in many fields.

1. Introduction

Recently, with the increasing serious problem of energy shortage, exploring a new pollution-free energy is urgently needed. Proton exchange membrane fuel cells (PEMFC) have become the focus of many researchers due to its advantages, such as high energy density, environmental friendliness and low pollution from combustion products [1–3]. Proton exchange membranes (PEM) play a pivotal role in proton conduction and simultaneously act as separator between fuel and oxidant, which can directly affect the performances of fuel cells [4]. Therefore, it is necessary to improve the quality of PEMs, such as high proton conductivity, better dimensional stability and outstanding anti-oxidation ability.

As a kind of high-performance engineering plastics, poly(arylene ether nitrile)s (PEN) possess excellent comprehensive properties of high-temperature resistance, radiation resistance, mechanical strength, molding and processing, which have broad application prospect in many fields [5–6]. To explore the use value of PEN as PEM, sulfonic acid groups were introduced into the main chain of PEN to synthetize a series of sulfonated poly(arylene ether nitrile)s (SPEN) with different structures. In previous works, the researchers found that the SPEN with large quantity of sulfonic acid groups possesses high proton conductivity, but may cause excessive swelling and poor dimensional stability [7]. That is to say, it is difficult for single SPEN to balance the relationship of various performances. Therefore, the fabrication of organic-inorganic hybrid composite membranes is an efficient approach to achieve excellent performances by combining the advantages of both organic and inorganic components.

Graphene oxide (GO) and multi-walled carbon nanotubes (MWCNT) have attracted extensive attention due to the superior properties such as low-weight, large specific surface area, high electrical conductivity,

extraordinary mechanical, optical, and thermal properties [8–9]. In the previous works, the adding of single GO (or MWCNT) as filler into SPEN matrix not only can greatly improve the proton transfer and impede methanol permeability, but also can significantly enhance the mechanical and thermal properties of PEMs [10–12]. As we know, hybrid fillers consisting of two or more different components may play synergistic enhancement effect on polymer matrix and endow better performances than single filler/polymer composites [13]. Zhang *et al*. reported the synergistic enhancement effects of mixed fillers composed of functionalized graphene and functionalized MWCNT on the electrical conductivity and tensile modulus of poly(ether sulfone) (PES) composites [14]. However, the complicated synthesis procedures limit the broad applications, while a simple, eco-friendly and inexpensive strategy is urgently needed for industrial applications. Divalent metal ions possess strong coordination ability for carboxyl, hydroxyl and other oxygen-containing functional groups. Among these, calcium ion (Ca^{2+}) attracts our attention for the low price, environmental friendly and extensive sources. The metal ions coordination not only can effectively bridge between GO and acidified MWCNT, forming three-dimensional structure, but also can be fitted with a variety of polymer matrices by π-π interaction [15–16], significantly improving the performances.

In this work, the calcium ion coordination GO and acidified MWCNT (GO-Ca^{2+}-MWCNT) was prepared and incorporated into SPEN to explore the effects of GO and MWCNT on dimensional stability, anti-oxidation ability and proton conductivity. The possible proton conducting process of the SPEN/GO-Ca^{2+}-MWCNT composite membranes was also proposed. It is proved that the three-dimensional structured GO and MWCNT bridged by Ca^{2+} exhibits a favorable synergistic enhancement effect, which could provide an alternative approach in clean energy production from environment-friendly sources.

2. Experimental Section

2.1 Materials

4,4'-biphenol (BP, AR), N-methylpyrrolidone (NMP, AR), potassium carbonate (K_2CO_3, AR) and ethanol were supplied by Chengdu Kelong Chemical Reagent Company. 2,6-Difluorobenzonitrile (DFBN) and potassium 2,5-dihydroxybenzenesulfonatetoluene (SHQ) were purchased from Sigma-Aldrich. Toluene was supplied by Chongqing Jiyuan Chemical Co., LTD. Sulfuric acid (H_2SO_4), phosphoric acid (H_3PO_4), potassium permanganate ($KMnO_4$), hydrogen peroxide (30%, H_2O_2), hydrochloric acid (HCl), nitric acid (HNO_3) and calcium chloride ($CaCl_2$) were purchased from Chengdu Haihong Chemical Reagent Company. Flake graphite was purchased from Nanjing Xianfeng Nanomaterials Technology Co., LTD, and multi-walled carbon nanotubes (MWCNT) were obtained from Chengdu Organic Research Institute, Chinese Academy of Sciences. All reagents were not further purified and treated before use. The SPEN matrix was synthesized via nucleophilic aromatic substitution reaction, according to the previous literatures [17–18]. GO was prepared by the modified Hummer's method [19].

2.2 Preparation of MWCNT

Acidified MWCNT was prepared by the traditional method of strong acid oxidation [20]. The detailed steps were as follows: 5 g MWCNT, 300 mL H_2SO_4 and 100 mL HNO_3 (volume ratio of 3:1) were mixed and slowly put into three-neck flask, vibrating by ultrasonic sound and stirring for 3 h at 60 ^oC. Then, the mixed solution was filtered and washed with deionized water until the PH=7. Finally, acidified MWCNT can be obtained after grinded and dried at 80 ^oC for 48 h.

2.3 Preparation of the GO-Ca^{2+}-MWCNT

GO (25 mg) and acidulated MWCNT (75 mg) (the mass ratio of GO and MWCNT is 3:1) were added into NMP solution (20 mL), vibrating by ultrasonic sound for 4 h to obtain homogeneous dispersion. Then, different amounts of $CaCl_2$ was added into the mixed solution, which the ratio of Ca^{2+} and C was controlled to be 0.001, 0.002, 0.004 and 0.006 mmol mg^{-1}, respectively, to explore the optimal Ca^{2+} concentration. The mixture was stirred simultaneously with sonication for 48 h at 45 ℃ to ensure the complete coordination of Ca^{2+} with GO and MWCNT. Finally, the GO-Ca^{2+}-MWCNT suspension was put into glass bottles in liquid nitrogen for preliminary frozen about 15 min, and transferred into vacuum freezing dryer at -40 ℃ for 48 h. The GO-Ca^{2+}-MWCNT with three-dimensional structure can be obtained. Besides, the blended particle of GO and MWCNT without Ca^{2+} coordination was also prepared for comparison based on above same method.

2.4 Fabrication of SPEN/GO-Ca^{2+}-MWCNT composite membranes

The SPEN/GO-Ca^{2+}-MWCNT composite membranes with different packing contents were prepared via solution-casting method. Firstly, the GO-Ca^{2+}-MWCNT filler was dispersed into NMP, ultrasounding for 6 h to form uniform dispersion. Meanwhile, a certain amount of SPEN and NMP were added into three-necked flask, heating and stirring to dissolve. Secondly, the above GO-Ca^{2+}-MWCNT dispersion was added into SPEN transparent solution with continuous stirring and sonication for 6 h at room temperature to integrate GO-Ca^{2+}-MWCNT and SPEN completely. After standing for 10 min, the solution was poured slowly onto clean and horizontal glass plate in the oven, following the temperature procedures of 80 ℃, 100 ℃, 120 ℃, each for 1 h, 160 ℃ and 200 ℃, each for 2 h. The membranes were cooled to room temperature naturally, and immersed into 1 M H_2SO_4 for 24 h. After washed repeatedly with deionized water and dried in the oven, the proton exchange composite membranes were obtained, and named as SPEN, SPEN/GO-Ca^{2+}-MWCNT-0.5, SPEN/GO-Ca^{2+}-MWCNT-1 and SPEN/GO-Ca^{2+}-MWCNT-2, respectively. The detailed preparation processes of GO-Ca^{2+}-MWCNT and SPEN/GO-Ca^{2+}-MWCNT composite membranes are shown in Fig. 1.

2.5 Characterizations

Fourier transform infrared (FTIR) spectra were recorded on Nicolet IS10 (Thermo Fisher, USA) in KBr pellets between 4000 and 400 cm^{-1}. UV-vis spectra were tested by uv-visible spectrophotometer (TU1800, China) in the wavelength range of 200-600 nm. Scanning electron microscope (SEM, FEI INSPECT F50,

USA) was used to observe the morphologies of GO-Ca^{2+}-MWCNT and all membranes. The membranes were fractured in liquid nitrogen and sprayed gold for 20 min. The thermogravimetric analysis was performed on TA Instruments Q50 (TA Instruments Ltd., USA) under N_2 atmosphere and the program was as follows: heating from room temperature to 150 ℃ at the rate of 10 ℃ min^{-1} to remove thermal history, and then cooling to room temperature naturally, heating to 600 ℃ at the rate of 20 ℃ min^{-1}. Mechanical properties of the membranes were conducted by the SANS microcomputer-controlled electronic universal testing machine (CMT6104) at fully dry state and room temperature. The sizes of sample were 1 cm×10 cm and the stretching rate was 5 mm min^{-1}. The oxidation stability of the membranes was measured the residual weight by soaking in Fenton's reagent (3 wt% H_2O_2 containing 4 ppm Fe^{2+}) for 8 h at 80 ℃. The water uptake (WU), swelling ratio (SR) and proton conductivity (σ) of the membranes were determined as reported literatures [21–23].

3. Results And Discussion

3.1 Optimal concentration of Ca^{2+}

To explore the optimal concentration of Ca^{2+} in GO-Ca^{2+}-MWCNT filler, Fig. 2 displays the dispersion states of GO-Ca^{2+}-MWCNT with different Ca^{2+}/C ratio (*i.e.*, 0.001, 0.002, 0.004 and 0.006 mmol mg^{-1}) in NMP solvent (20 mL), standing for 48 h. It is obvious that the dispersity becomes worse as the concentration increases. At 0.006 mmol mg^{-1} Ca^{2+}/C ratio, the particles precipitate completely, while remains disperse and stable at 0.001 mmol mg^{-1} Ca^{2+}/C ratio. Although high concentration ratio of Ca^{2+}/C provides larger probability to coordinate MWCNTs and GO by the oxygen-containing functional groups, the bad dispersion of GO-Ca^{2+}-MWCNT in NMP can also result in the bad dispersion in SPEN matrix. Therefore, 0.001 mmol mg^{-1} Ca^{2+}/C ratio was selected in this work.

3.2 Characterization of GO-Ca^{2+}-MWCNT

Figure 3 shows the FTIR spectra of MWCNT/GO and GO-Ca^{2+}-MWCNT. For GO/MWCNT, the spectra possess five distinct characteristic peaks, which are assigned to C=O (carboxyl/carbonyl) at 1628 cm^{-1}, C=C (aromatic ring) at 1579cm^{-1}, C-O (carboxyl) at 1400 cm^{-1}, C-O (epoxide/ether) at 1172 $cm^{-1}$and C-O (alkoxy) at 1079 cm^{-1}, respectively [24]. However, for GO-Ca^{2+}-MWCNT, the characteristic peak of C=O (carboxyl/carbonyl) at 1628 cm^{-1} disappears, and the peak of C-O (carboxyl) at 1400 cm^{-1} shifts to lower wavenumber, which is ascribed to the coordination of bivalent metal ions and carboxylic acids [25]. Besides, Figure 3 also shows that the intensity of C-O (epoxide/ether) band at 1172 cm^{-1} decreases and the intensity of C-O (alkoxy) band at 1079 cm^{-1} increases as compared with MWCNT/GO. This is due to the fact that the coordination of Ca^{2+} breaks the C-O band of epoxy groups and forms more alkoxy bonds [26]. All of these peaks provide evidences to the coordination of GO and MWCNT by Ca^{2+}.

Figure 4 shows the ultraviolet absorption spectra of MWCNT, GO, GO/MWCNT and GO-Ca^{2+}-MWCNT. Both GO and MWCNT exhibit one absorption peak between 200-300 nm due to the strong absorption of NMP solution, suggesting good dispersion of GO and MWCNT in NMP [24]. Besides, the peak at ~250 nm of GO-Ca^{2+}-MWCNT has obvious decrease, presumably due to the consumption of the C=O band, indicating the successful coordination of divalent metal ions and carboxylic acids. The similar conclusion has been obtained in previous literatures on Zn^{2+} and Cu^{2+} [27–28].

To intuitively observe the three-dimensional structure of GO-Ca^{2+}-MWCNT, the SEM morphologies of GO/MWCNT and GO-Ca^{2+}-MWCNT were characterized and showed in Fig. 5. As shown in Fig. 5a, the GO/MWCNT particle possesses no structural cross-linking between GO and MWCNT due to the simple blend of GO and MWCNT. Besides, the SEM image of GO/MWCNT has little differences with that of pure GO, which is ascribed to the fact that the nanoscale of acidified MWCNT is very small compared with GO. Fig. 5b exhibits that GO and MWCNT were cross-linked via bridge action to form three-dimensional structure, which can be seen clearly from the amplification area, as shown in Fig. 5c. SEM images demonstrate the successful coordination of the Ca^{2+} between GO and MWCNT. This structure provides more efficient transport pathways for protons to transfer in SPEN membranes.

TGA curves were used to characterize the weight loss of GO, MWCNT and GO-Ca^{2+}-MWCNT from room temperature to 600 ^{o}C under N_2 atmosphere, as shown in Fig. 6. From Fig. 6, the GO displays two significant weight loss states at about 100-200 ℃ and 200-600 ℃, respectively. One is the decomposition of oxygen-containing groups such as carboxyl, hydroxyl and epoxy groups, and the other is the splitting of carbon skeleton structure. The weight loss of MWCNT is about 14.58% from 200-600 ℃, proving that the surface of MWCNT also contains a certain amount of oxygen-containing groups such as hydroxyl and carboxyl. Besides, the curve of GO-Ca^{2+}-MWCNT also shows two significant decomposition states at about 100-230 ℃ and 230-600 ℃, respectively. The decomposition degree at about 100-230 ℃ has a slight decrease trend than that of GO, which is speculated to be the uncoordinated calcium ions crosslinking with oxygen-containing functional groups on GO and MWCNT. The second decomposition state at 230-600 ℃ is also the splitting of carbon skeleton structure. Therefore, the above results confirm that the GO and MWCNT were coordinated by calcium ions.

3.3 SEM Characterization of SPEN and composite membranes

Figure 7 shows the SEM images of pure SPEN and PEN/GO-Ca^{2+}-MWCNT-1 composite membrane. As shown in Fig. 7a, the morphology of SPEN is relative smooth, while the addition of GO-Ca^{2+}-MWCNT filler makes the cross-sectional of composite membranes rougher than pure SPEN, as shown in Fig. 7b. The GO-Ca^{2+}-MWCNT particles cannot cause obvious cracks or pinholes in composite membranes, indicating the excellent interfacial adhesion to SPEN matrix, which can be seen clearly from the marked rectangular boxed areas in Fig. 7b. Besides, Fig. 7b also well demonstrates that the particles possess better dispersion in SPEN matrix, which is the prerequisite for the better performances of composite

membranes. Therefore, the GO-Ca^{2+}-MWCNT particles with three-dimensional structure play an important role in improving the performances of SPEN-based composite membranes.

3.4 Thermal and mechanical stability of the membranes

Thermal stability and tensile properties are important factors to determine the performances of proton exchange membranes. Fig. 8 displays the TGA results of the SPEN and SPEN/GO-Ca^{2+}-MWCNT composite membranes. All the composites membranes exhibit two weight loss stages under N_2 atmosphere. The first stage at around 250 ℃ is related to the decomposition of sulfonic acid groups of SPEN and the organic groups of GO-Ca^{2+}-MWCNT [29]. The second stage at about 400 ℃ is attributed to the degradation of the main chain of SPEN and the carbon skeleton of GO-Ca^{2+}-MWCNT. As shown in Fig. 8, the weight losses of SPEN/GO-Ca^{2+}-MWCNT membranes at 250 ℃ and 400 ℃ are all lower than that of pure SPEN, suggesting that the sulfonic acid groups of SPEN can combine with the calcium ions of GO-Ca^{2+}-MWCNT, which can lead to higher thermal stability. Table 1 exhibits the thermogravimetric decomposition data of SPEN and SPEN-based composite membranes with different GO-Ca^{2+}-MWCNT contents. The 5% and 10% decomposition temperatures of composite membranes are higher than that of pure SPEN, and it increases with the increasing content, showing that the GO-Ca^{2+}-MWCNT can improve thermal stability of composite membranes, which validates the above results. In addition, the SPEN/GO-Ca^{2+}-MWCNT composites present same decomposition trends with SPEN, which can be considered that GO-Ca^{2+}-MWCNT as the filler has a positive impact on the thermal stability of SPEN-based composite membranes.

Table 1
The thermal stability of pure SPEN and SPEN/GO-Ca^{2+}-MWCNT composite membranes

Membranes	$T_{5\%}$ (℃)	$T_{10\%}$ (℃)	T_{max} (℃)
SPEN	311.50	354.45	369.51
SPEN/GO-Ca^{2+}-MWCNT-0.5	320.58	367.92	380.46
SPEN/GO-Ca^{2+}-MWCNT-1	326.74	371.18	371.22
SPEN/GO-Ca^{2+}-MWCNT-2	343.61	380.29	380.86

Table 2 presents the tensile strength and Young's modulus of pure SPEN and SPEN/GO-Ca^{2+}-MWCNT composite membranes at fully dry state and room temperature. The tensile strength and Young's modulus of the membranes increase from 62.41 to 71.45 MPa and from 1636.50 to 1715.09 MPa, respectively, as the GO-Ca^{2+}-MWCNT content increases to 1 wt%, which is attributed to the impediment of particles on the movement of polymer chain. The synergistic effect between calcium ions and SPEN also can enhance the tensile properties of the membranes [30]. However, the tensile strength and Young's modulus reduce to 63.88 MPa and 1643.37 MPa, respectively, as the GO-Ca^{2+}-MWCNT content increases to 2 wt%, which is due to the agglomeration phenomenon of excessive GO-Ca^{2+}-MWCNT particles. As

shown in Table 2, the tensile strength and Young's modulus of SPEN/GO-Ca^{2+}-MWCNT composites are higher than that of SPEN membrane, even in the composite membranes with high filler content, suggesting the outstanding enhancement effect of GO-Ca^{2+}-MWCNT to tensile properties of SPEN membrane.

Table 2
Mechanical stability of pure SPEN and SPEN/GO-Ca^{2+}-MWCNT composite membranes at room temperature

Membranes	Tensile strength (MPa)	Tensile modulus (MPa)
SPEN	62.41	1636.50
SPEN/GO-Ca^{2+}-MWCNT-0.5	64.12	1661.35
SPEN/GO-Ca^{2+}-MWCNT-1	71..45	1715.09
SPEN/GO-Ca^{2+}-MWCNT-2	63.88	1643.37

3.5 Oxidative stability of the membranes

Oxidation stability is vulnerable to judge the ability to resist free radicals of the membranes. All the membranes were soaked into Fenton's reagent (3 wt% H_2O_2 containing 4 ppm Fe^{2+}) for 8 h at 80 °C to simulate the environment of oxidative radicals attacking membranes, and then measure the residual weight percentages of the membranes. As shown in Table 3, the residual weight percentages of pure SPEN and SPEN/GO-Ca^{2+}-MWCNT composite membranes are 94.3%, 96.2%, 98.7% and 99.9%, respectively. The residual weight percentages of SPEN/GO-Ca^{2+}-MWCNT composite membranes are far higher than that of SPEN, and it increases with the increasing filler content, indicating that the GO-Ca^{2+}-MWCNT filler possesses excellent ability to resist free radicals, especially for the SPEN/GO-Ca^{2+}-MWCNT-2 membrane. This phenomenon can be explained by the following reasons. Firstly, GO possesses strong stability and oxidation resistance due to the large number of oxygen-containing functional groups, which can effectively resist the attack of oxidative free radicals [31–32]. Secondly, the oxygen-containing functional groups of GO-Ca^{2+}-MWCNT and SPEN can form hydrogen bonds interaction, enhancing the interfacial adhesion and resisting the oxidation of the membranes [33]. Finally, the interaction between the uncoordinated calcium ions of GO-Ca^{2+}-MWCNT and the SPEN also can function positively on the resistance to free radicals [32]. Therefore, the SPEN/GO-Ca^{2+}-MWCNT composite membranes possess excellent oxidation stability against Fenton's reagent.

Table 3

The oxidative stability, water uptake and swelling ratio of pure SPEN and SPEN/GO-Ca^{2+}-MWCNT composite membranes

Membranes	[a]Oxidative stability	WU (%)		SR (%)	
	[b]W (%)	30 ℃	80 ℃	30 ℃	80 ℃
SPEN	94.3	34.71	81.80	17.99	44.40
SPEN/GO-Ca^{2+}-MWCNT-0.5	96.2	34.88	50.17	17.74	38.42
SPEN/GO-Ca^{2+}-MWCNT-1	98.7	33.31	49.38	17.56	36.80
SPEN/GO-Ca^{2+}-MWCNT-2	99.9	32.27	45.77	16.11	36.40

[a] Measured at 80°C in Fenton's reagent (4 ppm $FeSO_4$ and 3% H_2O_2)

[b] Refers to the residual weight percentages of the membranes after soaked in Fenton's reagent (4 ppm $FeSO_4$ and 3% H_2O_2) for 8 h

3.6 Water uptake and swelling ratio of the membranes

Figure 9 and Table 3 present the water uptake and swelling ratio of SPEN and SPEN/GO-Ca^{2+}-MWCNT composite membranes at 30 ^oC and 80 ^oC, respectively. The water uptake and swelling ratio of SPEN/GO-Ca^{2+}-MWCNT composite membranes have a slight decrease compare with SPEN, which is due to the reduced free volume occupied by the inorganic filler [34]. The interaction between the sulfonic acid group of SPEN and uncoordinated calcium ions also can suppress the penetration of water molecules. Besides, temperature has a significant effect on the water uptake and swelling ratio, as shown in Figure 9. The water uptake and swelling ratio of all membranes at 80 ^oC are higher than that of 30 ^oC, which is caused by the increased transmission rate of water molecular and the formation of more hydronium ion (H_3O^+). Meanwhile, the influence on the water uptake and swelling ratio at 80 ^oC is greater than 30 ℃, which is mainly due to the fact that the water absorbing capacity of sulfonic acid groups of SPEN is weaker under low temperature conditions. It's worth noting that the swelling ratio of SPEN/GO-Ca^{2+}-MWCNT composite membranes is all less than 40% at 80 ℃, suggesting outstanding dimensional stability, speculating that the GO-Ca^{2+}-MWCNT particles limit the infinite expansion of the membranes.

3.7 Proton conductivity of the membranes

The influences of the GO-Ca^{2+}-MWCNT filler on the proton conduction properties of SPEN were also examined. Fig. 10 provides a comparison among the proton conductivity of pure SPEN and the three different kinds of SPEN composite membranes (filler contents=0.5, 1.0 and 2.0 wt%) at different temperatures and 100% humidity. Obviously, the proton conductivity of SPEN composite membranes rises with the increase content of GO-Ca^{2+}-MWCNT and reaches the maximum value at 1 wt%. The three-dimensional structured GO-Ca^{2+}-MWCNT provides more efficient channels for proton transmission and

increases proton transport efficiency [35]. However, the proton conductivity of SPEN/GO-Ca^{2+}-MWCNT-2 membrane has a downward trend, even lower than the SPEN. This is caused by the aggregation of excessive filler content, blocking the channels of proton transport in the membrane and then reducing greatly the efficiency of proton transport [36–37]. In addition, Fig. 10 exhibits that the proton conductivity of SPEN and composite membranes rises dramatically in the range of 30-90 ℃. The substantial increasing of water absorption can led to the sharp rise of proton conductivity due to the carrier effect of water molecules on proton conduction. Especially, the proton conductivity of SPEN/GO-Ca^{2+}-MWCNT-2 reaches the maximum of 0.193 S/cm at 90 ℃, 19.2% higher than that of SPEN, showing excellent proton transport capability. Therefore, the GO-Ca^{2+}-MWCNT filler with three-dimensional structure can significantly promote the proton conductivity of SPEN.

The enhancement effect on proton conduction of membranes can be explained by the Grotthuss mechanism. The surface of GO-Ca^{2+}-MWCNT filler still contains a large number of oxygen-containing functional groups, such as hydroxyl and uncoordinated carboxyl groups, which can form hydrogen bonds networks with the sulfonic acid groups of SPEN chain. According to the Grotthuss mechanism, the protons can be transferred from one carrier (sulfonic acid groups) to another (oxygen-containing functional groups) by the hydrogen bond networks. By this way, the continuous proton transports channels can be formed to accelerate proton transmission and trigger the synergistic enhancement effect between GO-Ca^{2+}-MWCNT and SPEN, improving the proton conductivity. The three-dimensional structured GO-Ca^{2+}-MWCNT can facilitate the construction of long-term and continuous proton transmission paths and accelerate the proton transfer rate in the composite membranes [38]. Beside, excellent interface adhesion provides a prerequisite for the proton transport.

4. Conclusions

Herein, the GO-Ca^{2+}-MWCNT was synthetized by coordination of calcium ions between GO and MWCNT to form three-dimensional structure, and then incorporated into SPEN as filler to fabricate SPEN/GO-Ca^{2+}-MWCNT proton exchange composite membranes. The three-dimensional structured GO-Ca^{2+}-MWCNT particles provided more efficient channels for proton transmission, resulting in the improvement of proton conduction, and synchronously endowed the excellent oxidation stability against Fenton's reagent to the composite membranes. The resulting composite membranes also exhibited better dispersion and interfacial compatibility with SPEN matrix, leading to enhanced thermal stability, tensile properties and dimensional stability. As a result, the SPEN/GO-Ca^{2+}-MWCNT-1 composite membrane presented the optimal performances, such as the strongest tensile strength of 71.45 MPa, and the highest proton conductivity (0.054 S/cm at 30 ℃, and 0.193 S/cm at 90 ℃), while maintaining better oxidation and dimensional stability. Therefore, a convenient and effective strategy was provided and confirmed to design high-performances SPEN-based composite membranes.

Declarations

Conflicts of Interest

The authors declare that they have no known competing financial interests or personal relationships that could have appeared to influence the work reported in this paper.

Acknowledgements

The authors wish to thank for financial support of this work from the Natural Science Foundation of the Jiangsu Higher Education Institutions of China (No. 20KJB430032), the Opening Project of Jiangsu Province Engineering Research Center of Agricultural Breeding Pollution Control and Resource (No. 2021ABPCR009), the school-level research projects of Yancheng Institute of Technology (No. xjr2019025), the Open Fund of National & Local Joint Engineering Research Center for Mineral Salt Deep Utilization (No. SF201902), the National Natural Science Foundation of China (No. 21805027), Sichuan Science and Technology Program (No. 2019YJ0197) and the Fundamental Research Funds for the Central Universities (ZYGX2019Z010).

References

1. X. Zhang, T. Zhang, H. Chen, Y. Cao, A review of online electrochemical diagnostic methods of on-board proton exchange membrane fuel cells. Appl. Energy **286**, 116481 (2021)
2. X. He, G.W. He, A. Zhao, W. Fei, Z. Jiang, Facilitating proton transport in Nafion-based membranes at low humidity by incorporating multifunctional graphene oxide nanosheets. ACS Appl. Mater. Interfaces **9**, 27676–27687 (2017)
3. X. Liu, J. Zhang, C. Zheng, J. Xue, T. Huang, Y. Yin, Oriented proton-conductive nano-sponge-facilitated polymer electrolyte membranes. Energy Environ. Sci. **13**, 297–309 (2020)
4. N. Ali, A. Said, F. Ali, M. Khan, Z.A. Sheikh, M. Bilal, Development and characterization of functionalized titanium dioxide–reinforced sulfonated copolyimide (SPI/TiO_2) nanocomposite membranes with improved mechanical, thermal, and electrochemical properties. J. Inorg. Organomet. Polym. **30**, 4585–04596 (2020)
5. H. Tang, P. Wang, P. Zheng, X. Liu, Core-shell structured $BaTiO_3$@polymer hybrid nanofller for poly(arylene ether nitrile) nanocomposites with enhanced dielectric properties and high thermal stability. Compos. Sci. Technol. **123**, 134–142 (2016)
6. Y. Zhan, X. Wan, S. He, Q. Yang, Y. He, Design of durable and efficient poly(arylene ether nitrile)/bioinspired polydopamine coated graphene oxide nanofbrous composite membrane for anionic dyes separation. Chem. Eng. J. **333**, 132–145 (2018)
7. M. Feng, Y. Huang, Y. Cheng, J. Liu, X. Liu, Rational design of sulfonated poly(ether ether ketone) grafted graphene oxide-based composites for proton exchange membranes with enhanced performance. Polymer **144**, 7–17 (2018)

8. N.G. Sahoo, S. Rana, J.W. Cho, L. Li, S.H. Chan, Polymer nanocomposites based on functionalized carbon nanotubes. Prog. Polym. Sci. **35**, 837–867 (2010)
9. W.W. Liu, S.P. Chai, A.R. Mohamed, U. Hashim, Synthesis and characterization of graphene and carbon nanotubes: a review on the past and recent developments. J. Ind. Eng. Chem. **20**, 1171–1185 (2014)
10. S. Gahlot, P.P. Sharma, V. Kulshrestha, P.K. Jha, SGO/SPES-based highly conducting polymer electrolyte membranes for fuel cell application. ACS Appl. Mater. Interfaces **6**, 5595–5601 (2014)
11. X. Qiu, T. Dong, M. Uedaa, X. Zhang, L. Wang, Sulfonated reduced grapheme oxide as a conductive layer in sulfonated poly(ether ether ketone) nanocomposite membranes. J. Membr. Sci. **524**, 663–672 (2017)
12. R. Kannan, B.A. Kakade, V.K. Pillai, Polymer electrolyte fuel cells using Nafion-based composite membranes with functionalized carbon nanotubes. Angew. Chem. Int. Ed. **47**, 2653–2656 (2008)
13. V.D. Punetha, S. Rana, H.J. Yoo, A. Chaurasia, J.T. McLeskey Jr., M.S. Ramasamy, N.G. Sahoo, J.W. Cho, Functionalization of carbon nanomaterials for advanced polymer nanocomposites: A comparison study between CNT and grapheme. Prog. Polym. Sci. **67**, 1–47 (2017)
14. S. Zhang, S. Yin, C. Rong, P. Huo, Z. Jiang, G. Wang, Synergistic effects of functionalized graphene and functionalized multi-walled carbon nanotubes on the electrical and mechanical properties of poly(ether sulfone) composites. Eur. Polym. J. **49**, 3125–3134 (2013)
15. Y.-T. Liu, X.-M. Xie, X.-Y. Ye, High-concentration organic solutions of poly(styrene-co-butadiene-co-styrene)-modified graphene sheets exfoliated from graphite. Carbon **49**, 3529–3537 (2011)
16. Y.-T. Liu, X.-M. Xie, Y.-F. Gao, Q.-P. Feng, L.-R. Guo, X.-H. Wang, X.-Y. Ye, Polymer-assisted assembly of carbon nanotubes via a template-based method. Carbon **44**, 599–602 (2006)
17. M. Feng, Y. You, P. Zheng, J. Liu, K. Jia, Y. Huang, X. Liu, Low-swelling proton conducting multi-layer, composite membranes containing polyarylene ether nitrile and sulfonated carbon nanotubes for fuel cells. Int. J. Hydrogen Energy **41**, 5113–5122 (2016)
18. Y. Gao, G.P. Robertson, M.D. Guiver, S.D. Mikhailenko, X. Li, S. Kaliaguine, Synthesis of copoly(aryl ether ether nitrile)s containing sulfonic acid groups for PEM application. Macromolecules **38**, 3237–3245 (2005)
19. D.C. Marcano, D.V. Kosynkin, J.M. Berlin, A. Sinitskii, Z.Z. Sun, A. Slesarev, L.B. Alemany, W. Lu, J.M. Tour, Improved synthesis of graphene oxide. ACS Nano **4**, 4806–4814 (2010)
20. F. Jin, M. Feng, X. Huang, C. Long, K. Jia, X. Liu, Effect of SiO_2 grafted MWCNTs on the mechanical and dielectric properties of PEN composite films. Appl. Surf. Sci. **357**, 704–711 (2015)
21. P. Chen, L. Hao, W. Wu, Y. Li, J. Wang, Polymer-inorganic hybrid proton conductive membranes: Effect of the interfacial transfer pathways. Electrochim. Acta **212**, 426–439 (2016)
22. M.T. Taghizadeh, M. Vatanparast, Ultrasonic-assisted synthesis of ZrO_2 nanoparticles and their application to improve the chemical stability of Nafion membrane in proton exchange membrane (PEM) fuel cells. J. Colloid Interface Sci. **483**, 1–10 (2016)

23. D.W. Shin, S.Y. Lee, N.R. Kang, K.H. Lee, M.D. Guiver, Y.M. Lee, Durable sulfonated poly(arylene sulfide sulfone nitrile)s containing naphthalene units for direct methanol fuel cells (DMFCs). Macromolecules **46**, 3452–3460 (2013)
24. Y. Liu, Q. Feng, X. Xie, X. Ye, The production of flexible and transparent conductive films of carbon nanotube/graphene networks coordinated by divalent metal (Cu, Ca or Mg) ions. Carbon **49**, 3371–3391 (2011)
25. S. Park, K.-S. Lee, G. Bozoklu, W. Cai, S.T. Nguyen, R.S. Ruoff, Graphene oxide papers modified by divalent ions-enhancing mechanical properties via chemical cross-linking. ACS Nano **2**, 572–578 (2008)
26. A. Lerf, H. He, M. Forster, J. Klinowski, Structure of graphite oxide revisited. J. Phys. Chem. B **102**, 4477–4482 (1998)
27. R. Wei, J. Wang, H. Zhang, W. Han, X. Liu, Crosslinked polyarylene ether nitrile interpenetrating with Zinc ion bridged graphene sheet and carbon nanotube network. Polymers **9**, 342 (2017)
28. L. Tong, R. Wei, J. Wang, X. Liu, Phthalonitrile end-capped polyarylene ether nitrile nanocomposites with Cu^{2+} bridged carbon nanotube and graphene oxide network. Mater. Lett. **178**, 312–315 (2016)
29. J. Maiti, N. Kakati, S.P. Woo, Y.S. Yoon, Nafion based hybrid composite membrane containing GO and dihydrogen phosphate functionalized ionic liquid for high temperature polymer electrolyte membrane fuel cell. Compos. Sci. Technol. **155**, 189–196 (2018)
30. J.Y. Kong, M.C. Choi, G.Y. Kim, J.P. Jin, M. Selvaraj, M. Han, C.S. Ha, Preparation and properties of polyimide/graphene oxide nanocomposite films with Mg ion crosslinker. Eur. Polym. J. **48**, 1394–1405 (2012)
31. K. Kim, J. Bae, M.-Y. Lim, P. Heo, S.-W. Choi, H.-H. Kwon, J.-C. Lee, Enhanced physical stability and chemical durability of sulfonated poly (arylene ether sulfone) composite membranes having antioxidant grafted graphene oxide for polymer electrolyte membrane fuel cell applications. J. Membr. Sci. **525**, 125–134 (2017)
32. R.P. Pandey, V.K. Shahi, Sulphonated imidized graphene oxide (SIGO) based polymer electrolyte membrane for improved water retention, stability and proton conductivity. J. Power Sources **299**, 104–113 (2015)
33. A.U. Devi, K. Divya, N.J. Kaleekkal, D. Rana, A. Nagendran, Tailored SPVdF-co-HFP/SGO nanocomposite proton exchange membranes for direct methanol fuel cells. Polymer **140**, 22–32 (2018)
34. T. Ko, K. Kim, M.-Y. Lim, S.Y. Nam, T.-H. Kim, S.-K. Kim, J.-C. Lee, Sulfonated poly(arylene ether sulfone) composite membranes having poly(2,5-benzimidazole)-grafted graphene oxide for fuel cell applications. J. Mater. Chem. A **3**, 20595–20606 (2015)
35. W. Jia, B. Tang, P. Wu, Novel slightly reduced graphene oxide based proton exchange membrane with constructed long-range ionic nanochannels via self-assembling of Nafion. ACS Appl. Mater. Interfaces **9**, 22620–22627 (2017)

36. Y. Yin, H. Wang, L. Cao, Z. Li, Z. Li, M. Gang, C. Wang, H. Wu, Z. Jiang, P. Zhang, Sulfonated poly(ether ether ketone)-based hybrid membranes containing graphene oxide with acid-base pairs for direct methanol fuel cells. Electrochim. Acta **203**, 178–188 (2016)
37. V. Parthiban, S. Akula, S.G. Peera, N. Islam, A.K. Sahu, Proton conducting Nafion-sulfonated graphene hybrid membranes for direct methanol fuel cells with reduced methanol crossover. Energy Fuels **30**, 725–734 (2016)
38. M. Feng, Z. Pu, P. Zheng, K. Jia, X. Liu, Sulfonated carbon nanotubes synergistically enhanced the proton conductivity of sulfonated polyarylene ether nitriles. RSC Adv. **5**, 34372–34376 (2015)

Figures

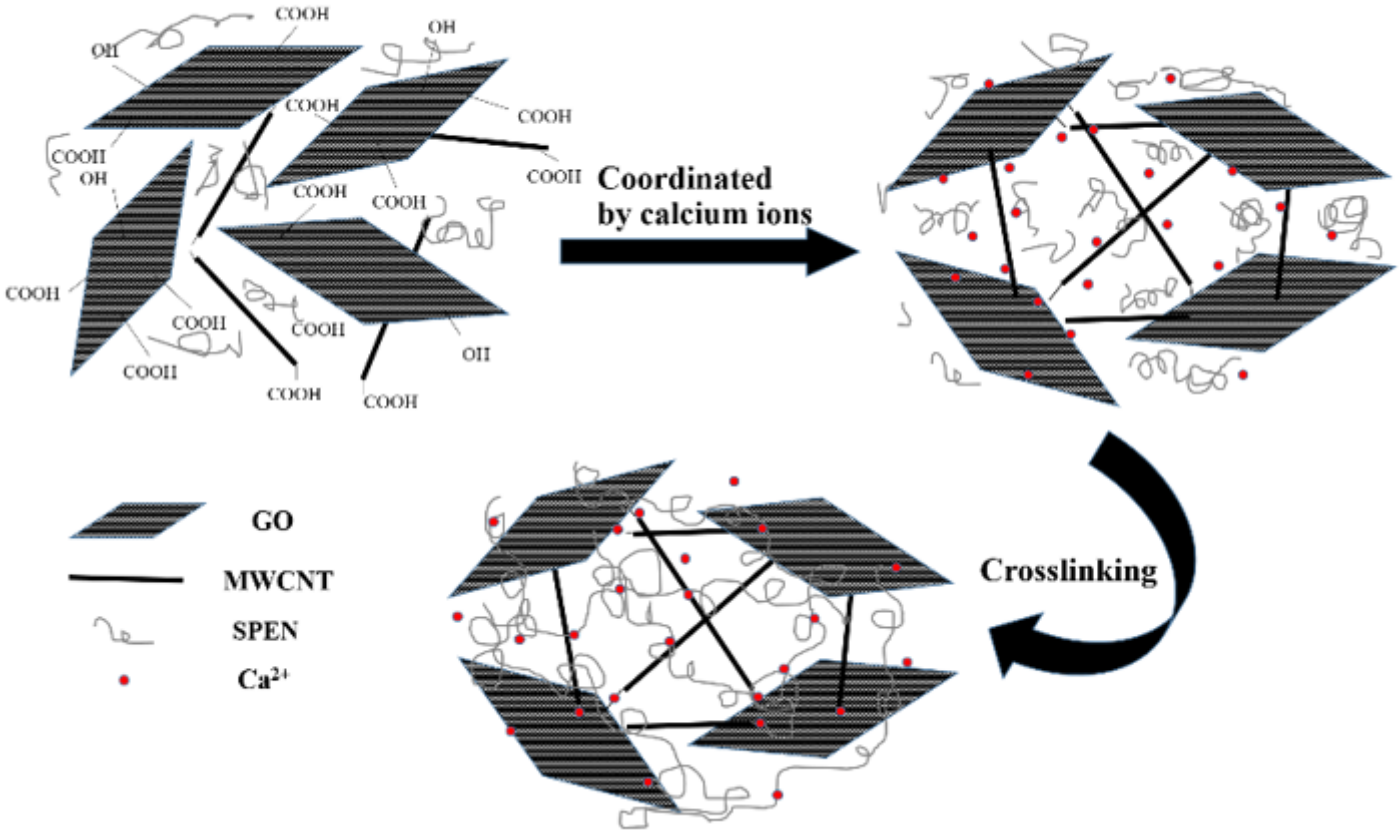

Figure 1

The detailed preparation processes of GO-Ca^{2+}-MWCNT and SPEN/GO-Ca^{2+}-MWCNT composite membranes

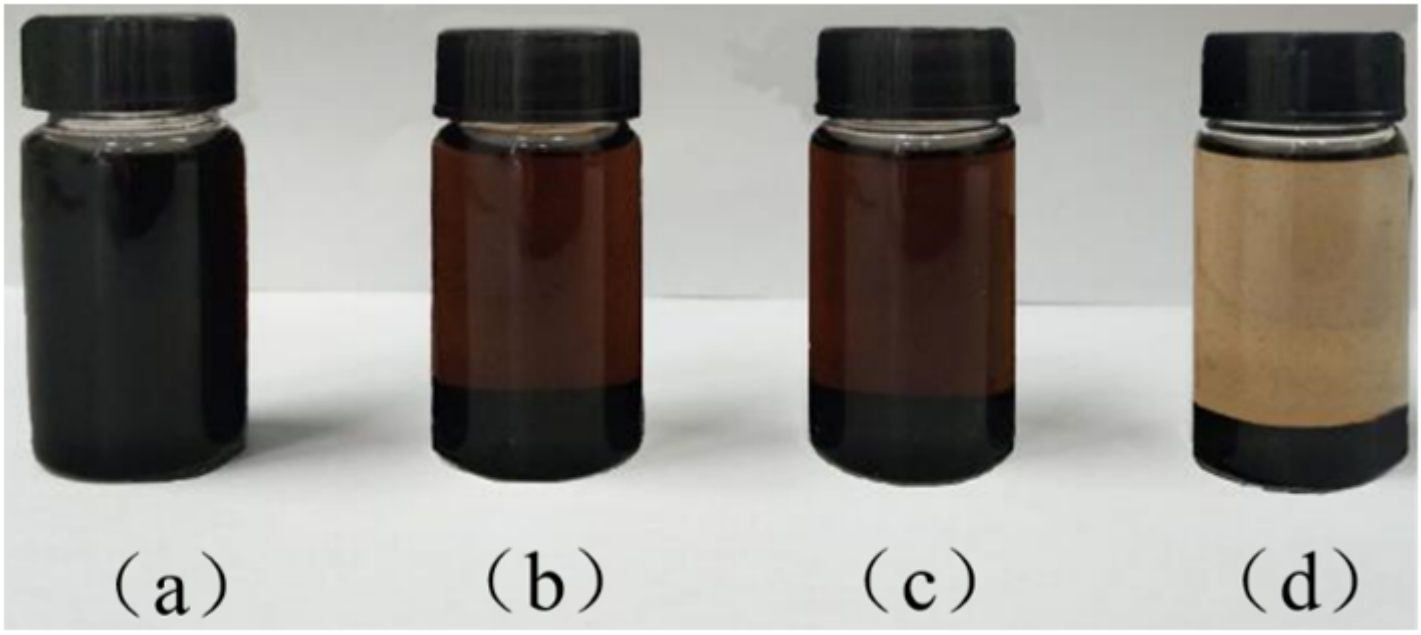

Figure 2

The dispersion states of GO-Ca^{2+}-MWCNT with different Ca^{2+}/C ratio, (a) 0.001, (b) 0.002, (c) 0.004 and (d) 0.006 mmol mg^{-1} in NMP solvent

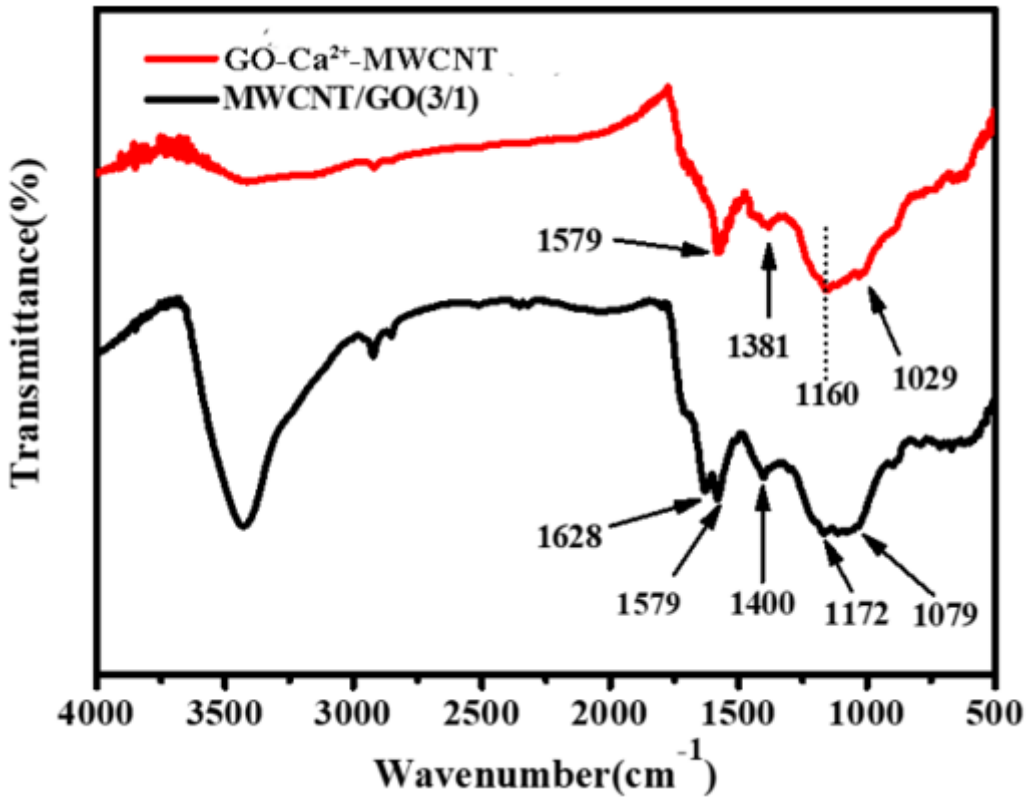

Figure 3

FTIR spectra of MWCNT/GO (3/1) and GO-Ca^{2+}-MWCNT

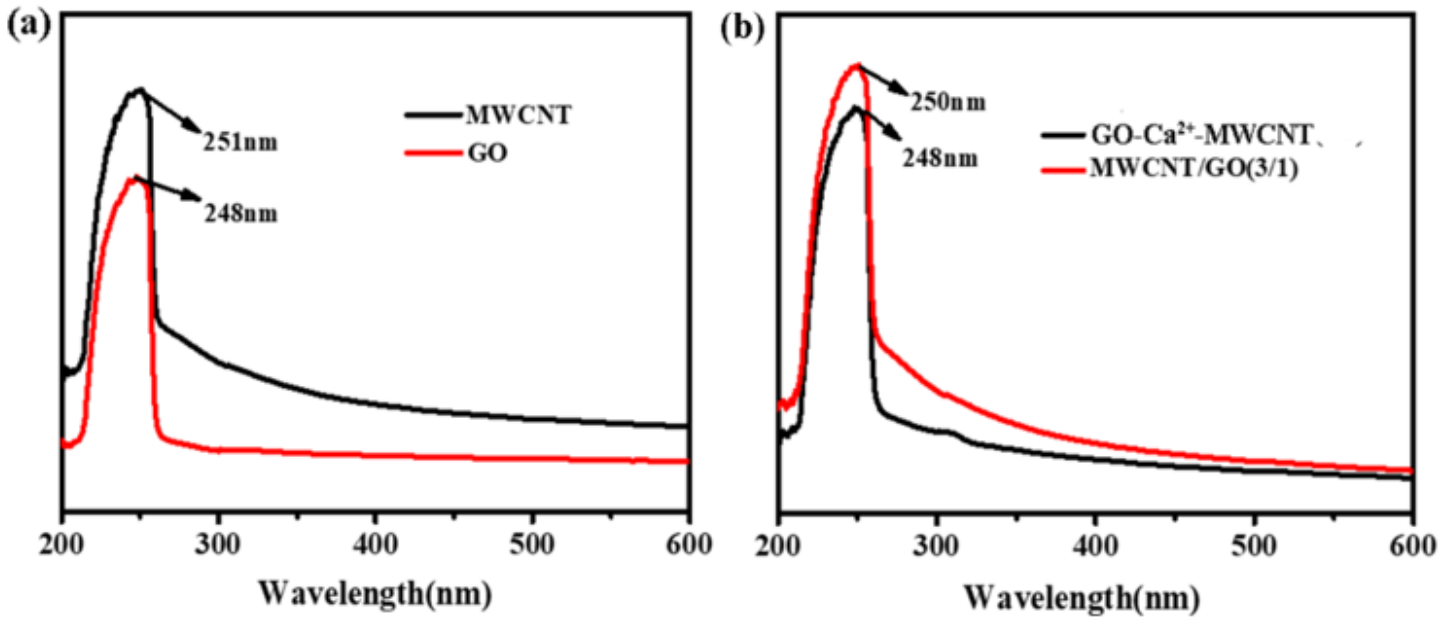

Figure 4

UV-vis spectra of (a) MWCNT, GO, (b)GO/MWCNT and GO-Ca^{2+}-MWCNT

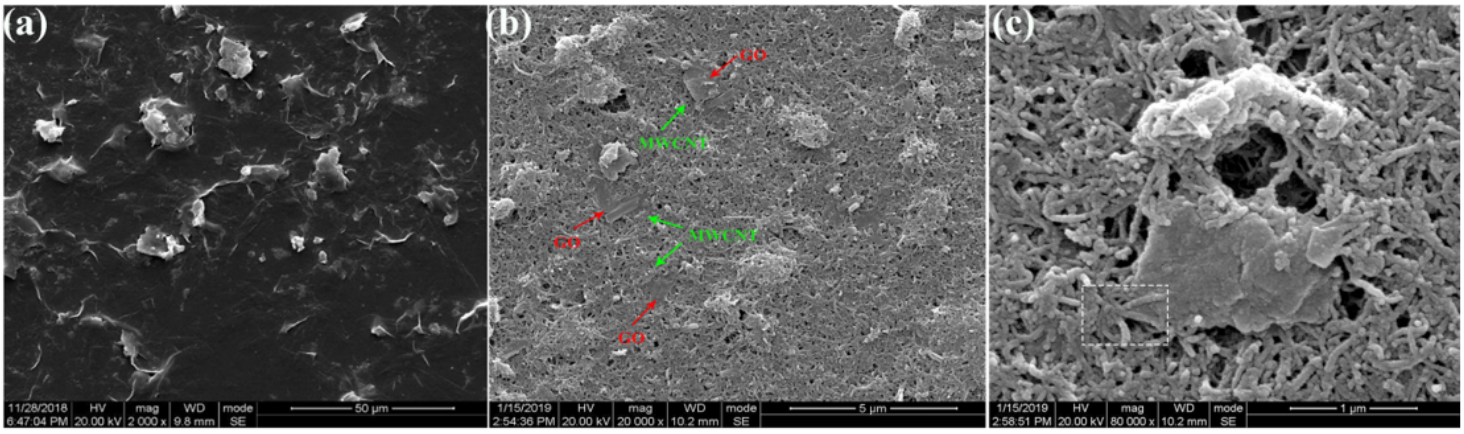

Figure 5

SEM images of (a) GO/MWCNT and (b, c) GO-Ca^{2+}-MWCNT at the scale bar of 5 μm and 1 μm, respectively

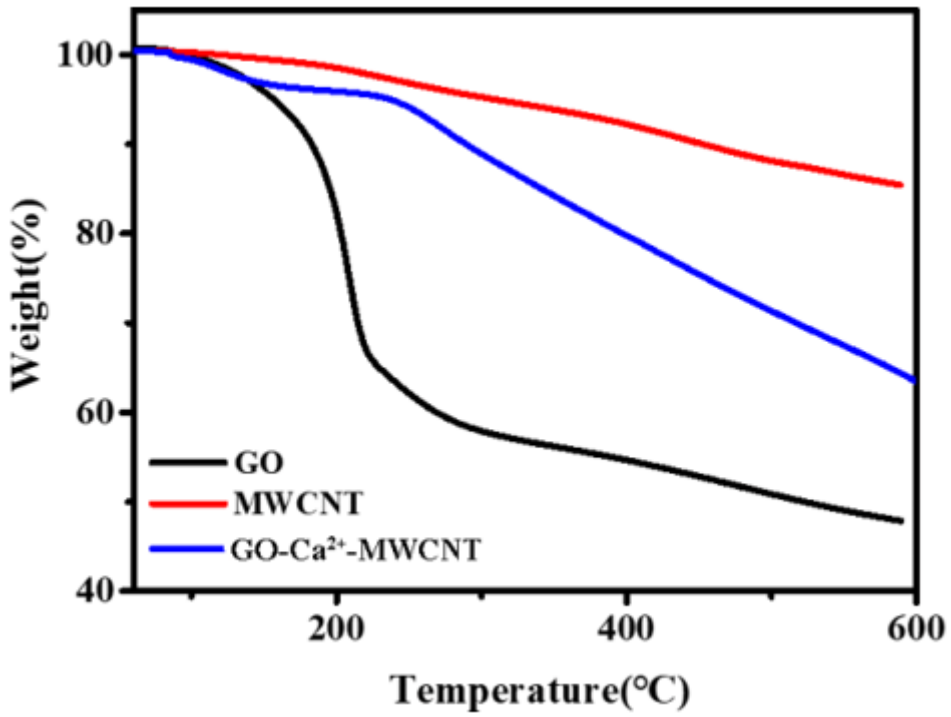

Figure 6

TGA curves of GO, MWCNT and GO-Ca^{2+}-MWCNT

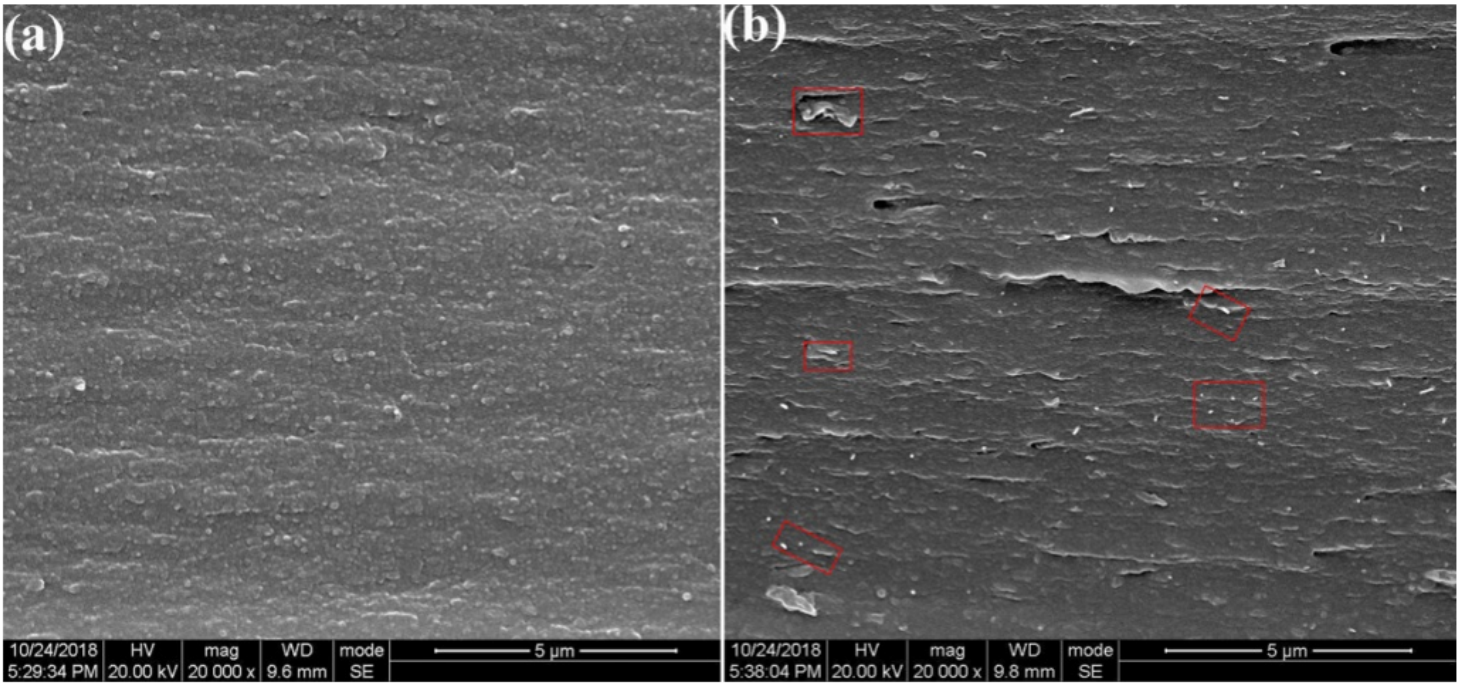

Figure 7

The cross-sectional SEM images of (a) Pure SPEN, (b) SPEN/GO-Ca^{2+}-MWCNT-1 composite membrane

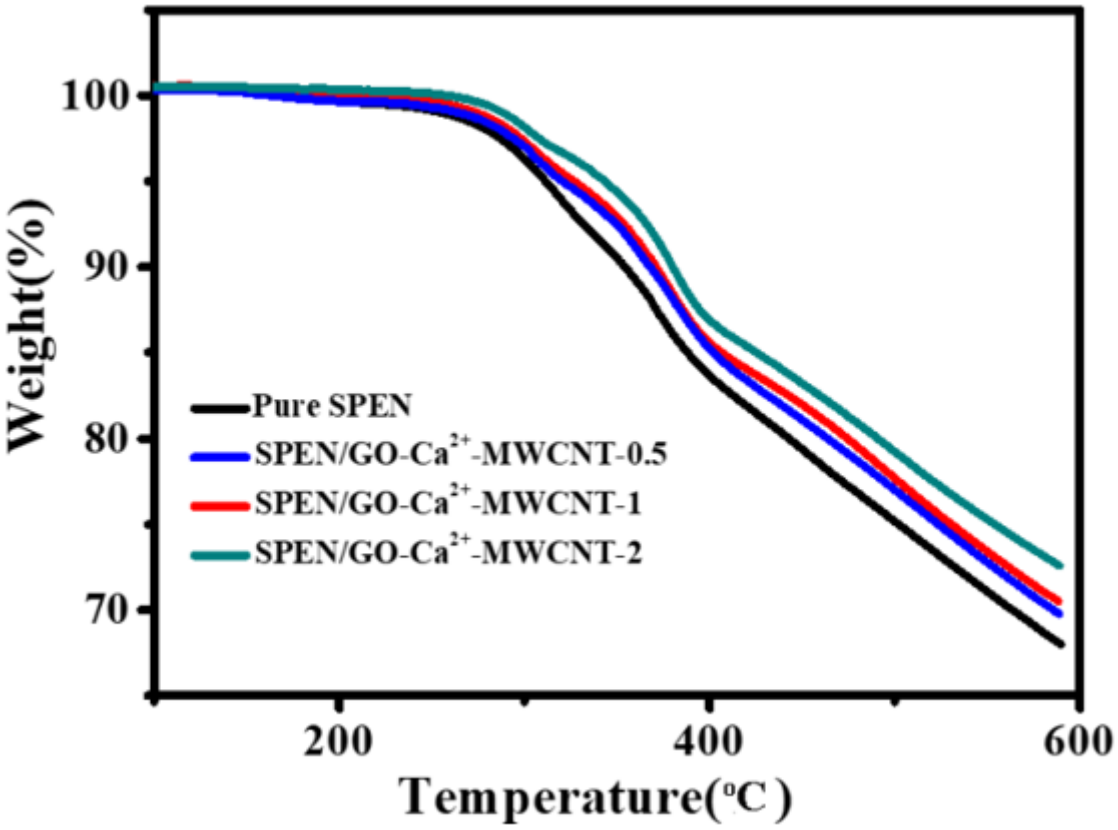

Figure 8

TGA curves of pure SPEN and SPEN/GO-Ca^{2+}-MWCNT composite membranes

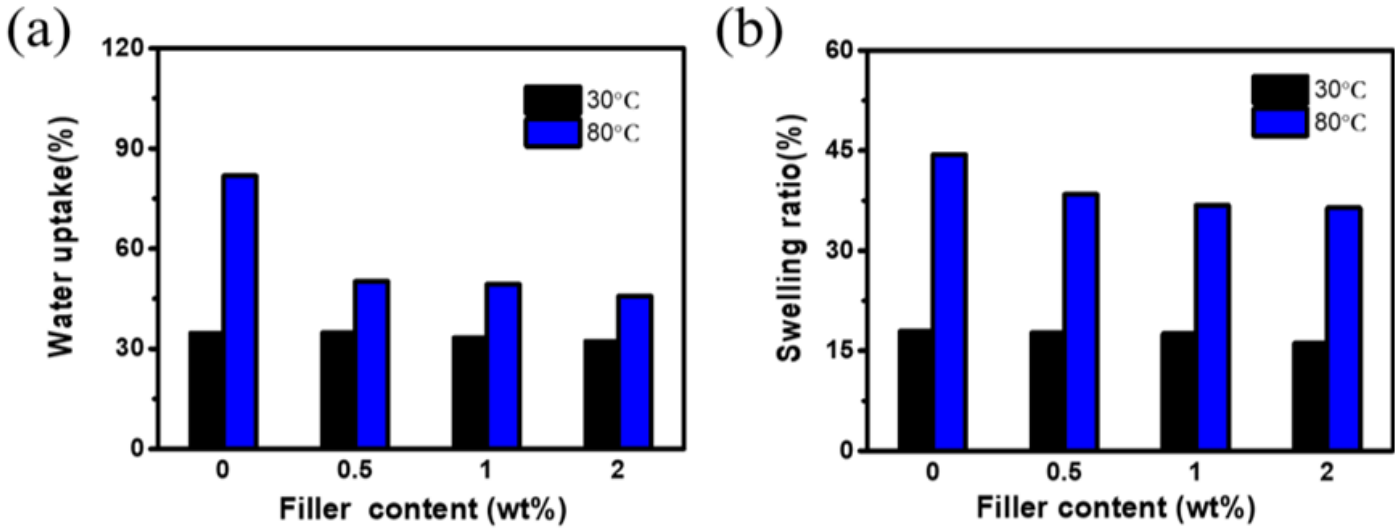

Figure 9

Water uptake and swelling ratio of pure SPEN and SPEN/GO-Ca^{2+}-MWCNT composite membranes at 30 ^{o}C and 80 ^{o}C, respectively

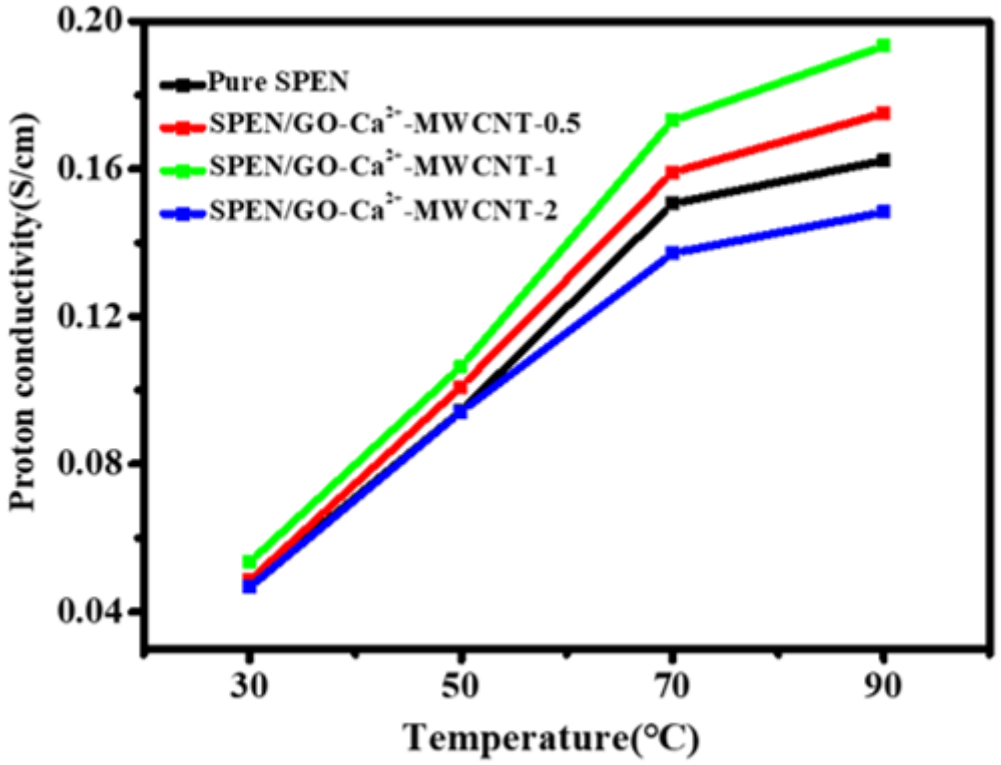

Figure 10

Proton conductivity of pure SPEN and SPEN/GO-Ca^{2+}-MWCNT composite membranes at different temperatures